Climate Dynamics (2021) 57:657–669
https://doi.org/10.1007/s00382-021-05731-x

Influence of the QBO on tropical convection and its impact on tropical cyclone activity over the western North Pacific

Jingliang Huangfu[1] · Yulian Tang[1,2] · Tianjiao Ma[1] · Wen Chen[1] · Lin Wang[1]

Received: 26 October 2020 / Accepted: 9 March 2021 / Published online: 18 March 2021

Abstract

On the basis of 70 hPa zonal wind (U70)-defined quasi-biennial oscillation (QBO) events, after removing the El Niño–Southern Oscillation (ENSO) signal, the present study investigates the process by which the QBO modulates tropospheric circulation and convection during summer (between July and October), when tropical cyclone (TC) activities enter their peak period. Concurrent with the western phase of the QBO (QBOW), significant tripole pattern modulations over the tropical Indo-Pacific Ocean are regressed onto the residual part of U70 after removing the ENSO signal, with enhanced convection observed over its central branch (0°–10°N, 120°E–180°) and the inactive convection branches located to both sides. A ventilation opening-like effect is exerted on the monsoon trough, which is shifted southward under the QBOW phase. According to the QBO-associated changes in the circulations over the tropical western North Pacific (WNP), equatorial environments (with low-level relative vorticity, high-level divergence, tropospheric vertical wind shear (VWS), and midlevel humidity) tend to be favorable for TC genesis. Consequently, the off-equatorial TC tracks show a significantly decreased occurrence frequency in the northern monsoon trough region. The present study provides a summary sketch showing the QBO-tropospheric circulation modulation process. Considering that the westerly or weak easterly is observed over the upper central Pacific (CP), QBOW phase-associated weak VWS can induce anomalous upward motion at equatorial latitudes, together with the upwelling between the equatorial westerly and off-equatorial easterly, leading to an enlarged convective window over the CP. Affected by the prevailing easterly within the tropics, the actual pumping shifts westward over the tropical WNP.

Keywords Quasi-biennial oscillation · Tropical convection · Tropical cyclone activity · Western North Pacific

1 Introduction

The quasi-biennial oscillation (QBO) is the most stable periodic (period of approximately 28 months) phenomenon observed in the lower stratosphere (16–50 km); the QBO is especially notable in the zonal winds over the equator shifting between the westerlies (QBOW) and the easterlies (QBOE) (Reed et al. 1961; Angell and Korshover 1964; Baldwin et al. 2001). The QBO signal propagates downward in the lower stratosphere, maintaining a nearly constant amplitude above 40 hPa, and the signal dominates the deep lower stratosphere to 70 hPa (Reed et al. 1961; Baldwin et al. 2001). Some years exhibit a significant vertical wind shear (VWS) between 30 and 70 hPa, with a westerly (easterly) shear meaning that westerly (easterly) winds increase with height (Baldwin et al. 2001). Therefore, conclusions based on different levels or descriptions of the QBO may result in confusion; for example, 30 hPa westerlies generally correspond to 70 hPa easterlies (e.g., Gray et al. 1992; Chan 1995; Huesmann and Hitchman 2001; Camargo and Sobel 2010; Xue et al. 2015).

Previous studies investigated the influence of the QBO on tropical cyclone (TC) activity (Gray 1984; Shapiro 1989; Chan 1995; Ho et al. 2009). Pioneering work was conducted by Gray (1984), who connected the QBO to Atlantic TC activity and employed the QBO signal as a predictor in TC seasonal forecasts. In QBOW (30 hPa) years, the seasonal numbers of hurricanes, hurricane days and tropical storms are above normal levels (Gray 1984). Furthermore, approximately 30% of the total variance of Atlantic TC activity is

✉ Lin Wang
wanglin@mail.iap.ac.cn

[1] Center for Monsoon System Research, Institute of Atmospheric Physics, Chinese Academy of Sciences, Beijing, China

[2] College of Earth and Planetary Sciences, University of Chinese Academy of Sciences, Beijing 100049, China

explained by the QBO (30 hPa), and the 50 hPa QBO signal can show a direct correlation with TC frequency based on extrapolation (Shapiro 1989). Similar studies were conducted between the QBO and TC activity over the western North Pacific (WNP) (Gray et al. 1992; Chan 1995). In QBOW (50, 30 and 10 hPa) years, more TCs are generated over the WNP than in QBOE years, where TCs with greater intensity show more robust correlations (Chan 1995). These studies mentioned that a similar correlation exists between El Niño–Southern Oscillation (ENSO) events and TC anomalies, but that it is independent of the QBO–TC correlation. Moreover, Camargo and Sobel (2010) revisited the QBO (30 hPa)-TC correlation globally; after removing ENSO signals, they suggested that the QBO–TC relationship shows significant interdecadal variations before and after the 1980s, which is partly attributed to the onset of the satellite era in 1979. In the record after the 1980s, only the central Pacific (CP) region shows a significant QBO–TC correlation. However, Camargo and Sobel (2010) questioned this correlation mathematically, considering that only a small number of TCs were generated in this region. Given the longer availability of satellite data, we can now reexamine the QBO–TC relationship for the whole Pacific basin based on an analysis of the QBO–troposphere interaction process.

Potential mechanisms for the QBO–troposphere interaction process have been extensively discussed (Gray 1988; Gray et al. 1992; Chan 1995; Collimore et al. 2003; Ho et al. 2009; Fadnavis et al. 2011, 2014; Huang et al. 2012; Liang et al. 2012; Zhang et al. 2019; Lee et al. 2019). Gray et al. (1992) interpreted the tropical route for the QBO–troposphere interaction process as follows: in QBOW (30 hPa) years, horizontally, westerlies dominate the equatorial region, while easterlies prevail in the boreal tropics during summer. The cyclonic circulation in the tropical lower stratosphere can lead to cross-tropopause upwelling vertical motion over the off-equatorial regions; vertically, westerlies in the lower stratosphere and easterlies in the upper troposphere result in a large VWS along the equator, which suppresses the deep convection at the equator. Hence, reversed Hadley circulation anomalies are aroused in QBOW years. Note that the QBOW phase discussed here should be interpreted as a deep and idealized system throughout the lower stratosphere; this configuration changes if the westerly phase is confined above 30 hPa. Collimore et al. (2003) summarized three mechanisms linking the QBO to tropical deep convection: tropopause height modulation, cross-tropopause wind shear modulation and relative vorticity modulation. According to Gray (1988), environmental influences on TCs include not only stratospheric influence, but also influences of the surface and surrounding system. The present study will analyze the QBO-associated surface and surrounding system affecting TCs, providing supplementary explanation regarding the QBO–TC modulation. Moreover, mechanisms of the QBO–TC track modulation have also been investigated in previous studies (e.g., Ho et al. 2009; Fadnavis et al. 2011, 2014). Ho et al. (2009) attributed QBO–TC track modulation to the background flow. Further, Fadnavis et al. (2014) proposed a mechanism through which the QBO-modulated steering winds can redistribute TC-associated deep convection and thus influence TC tracks. As the most important background in TC peak season, changes in monsoon trough are investigated in the present study. Further, we have included the calculation of accumulated cyclone energy (ACE; Bell et al. 2000) to show the QBO influence on TC strength.

Huang et al. (2012) suggest that the modulation of the Walker circulation and deep convection changes by QBO (30 hPa) depends upon atmospheric stability near the tropopause, which is affected by the cross-tropopause temperature difference. Their results further showed that enhanced atmospheric stability anomalies are observed over the CP in QBOW years, which is consistent with the analysis in Gray et al. (1992). However, the zonal differences of tropospheric responses, including vertical motion anomalies, energy conversions and mid-level tropospheric humidity, focusing on the QBO-induced changes affecting TC activities, still need further investigation.

Recently, Gray et al. (2018) reported another systematic work on the QBO employing 70 hPa as the critical level for the QBO (Gray et al. 2018). In QBOW (70 hPa) years, to maintain thermal wind balance in the presence of strong VWS at equatorial latitudes, a corresponding meridional circulation is induced, with anomalous downwelling over the equator and enhanced convection locating at off-equatorial latitudes. Therefore, increased summertime precipitation occurs over the tropical western Pacific (WP) under the QBOW phases (e.g., Giorgetta et al. 1999; Ho et al. 2009). Gray et al. (2018) showed that the 70 hPa zonal wind (hereafter referred to as U70) is a better predictor than the conventional 30 hPa zonal wind when studying the QBO-tropical deep convection relationship. Moreover, they suggested that the 70-hPa QBO is more consistent with the aforementioned QBO–troposphere mechanisms (Gray et al. 1992; Baldwin et al. 2001; Collimore et al. 2003). Therefore, it is necessary to reexamine the QBO–TC relationship in the Pacific using U70 to explain the process more clearly.

This study is structured as follows. The datasets and methods used in this study are described in Sect. 2. In Sect. 3, we examine the QBO-tropospheric circulation anomalies in the tropics. Subsequently, we show the modulation of the QBO on the TC activities over the WNP in Sect. 4. Section 5 summarizes this study and discusses its potential value for future works concerning the QBO–troposphere interaction process.

2 Data and Methods

2.1 Data

(1) Observational zonal winds at 50 hPa (U50) and U70 during the period from 1979 to 2018 are obtained from the Free University of Berlin (FUB-qbo; available at http://www.geo.fu-berlin.de/met/ag/strat/produkte/qbo/qbo.dat). These well-known QBO data are based on radiosonde observations in Singapore (1.22° N, 103.55° E). Considering that the QBO is zonally homogeneous and centered on the equator (Belmont and Dartt 1968; Wallace 1973), these single-station observations can represent the zonal winds in the lower stratosphere over the whole equator.

(2) The ERA-Interim Reanalysis dataset provides both tropospheric and stratospheric wind (horizontal and vertical) data, which are employed in the present study to explain the QBO–troposphere interaction process from a dynamic perspective. These reanalysis data are highly consistent with the aforementioned observational data and have been examined in many previous studies (e.g., Huangfu et al. 2019b). Additionally, this dataset provides monthly sea level pressure, air temperature, relative humidity, relative vorticity, divergence, and surface pressure data during 1979–2018 at a 2.5° × 2.5° resolution (Simmons et al. 2007; available at https://apps.ecmwf.int/datasets/data/interim-full-moda/levtype=sfc/).

(3) TC data from the International Best Track Archive for Climate Stewardship (IBTrACS; data version: v04r00), developed by the National Oceanic and Atmospheric Administration (NOAA), are used in this study; we employed data between 1979 and 2018 (Knapp et al. 2010, 2018). This newly released dataset provides updated TC data by integrating the World Meteorological Organization (WMO)-reported information into the IBTrACS files, providing wind speeds and central pressures as averages, which can be downloaded at https://www.ncdc.noaa.gov/ibtracs/. The interannual numbers of TCs in the present study are counted during the season when TCs are generated most frequently (July–August–September–October; JASO) at three levels: tropical depression (TD), tropical storm (TS; above 34 knots), and typhoon (TY; above 64 knots). Considering that the WMO data are official data from a responsible agency, we defined the TC genesis locations according to the WMO-reported identity numbers.

(4) The outgoing longwave radiation (OLR) is a good proxy for the tropical deep convection and can similarly be obtained from the NOAA archives (Liebmann 1996). Interpolated monthly mean OLR data with 2.5° × 2.5° resolution are provided; for this study, data during 1979–2018 are extracted and analyzed (available at https://psl.noaa.gov/data/gridded/data.interp_OLR.html).

(5) Monthly sea surface temperature (SST; HadISST) data from 1979 to 2018 at 1° × 1° resolution are provided by the Met Office Hadley Centre (Rayner et al. 2003).

2.2 Methods

In this study, we employed the observational U70 as the QBO signal following the work of Gray et al. (2018). Further comparisons and analyses between U50 and U70 are described in Sect. 3. The wavelet analysis method is applied to U70 to verify its capacity to represent the QBO. Considering that a specific year could be defined as a QBO year or an ENSO event based on the aforementioned indices at the same time, simply omitting El Niño and La Niña years from the record not only removes the ENSO signal but also removes the QBO signal. Therefore, we attempted to remove the monthly ENSO signal (Niño3.4 index employed in the present study) from the original data including tropical convection, atmospheric circulations and TC-related environmental factors by partial regression following previous studies (Wang et al. 2007; Chen et al. 2013). All of the datasets were preprocessed monthly using the following calculation:

$$A_{res} = A - rc(A, Niño\ 3.4\ Index) \times Niño\ 3.4\ Index$$

where A_{res} denotes the residual part of variable A after removing the monthly ENSO signal, and rc denotes the regression coefficient.

Similarly, the QBOW (QBOE) phase is identified when the normalized U70res averaged for JASO is greater (less) than 0.6 (− 0.6), where U70res is the residual part of U70. Normalization is conducted by dividing the anomalies by the standard deviation of the JASO-mean time series. The selection of this threshold (0.6) aims mainly to provide as many examples as possible, and the composite analysis results are not sensitive to this selection. Based on this threshold, composite analyses are further conducted to determine the differences in the monsoon trough (MT) and TCs generated over the WNP under the phases of both QBOW and QBOE. Statistically significant differences are assessed using Student's *t* test.

In addition, we calculated the genesis potential index (GPI), which reflects the potential of TC genesis. The GPI (Emanuel and Nolan 2004; Camargo et al. 2007) is calculated as follows:

$$GPI = \left|10^5\eta\right|^{3/2}\left(\frac{H}{50}\right)^3\left(\frac{V_{pot}}{70}\right)^3(1+0.1V_{shear})^{-2}$$

where η denotes the absolute vorticity at 850 hPa, and H denotes the relative humidity at 600 hPa. V_{pot} denotes the

potential intensity derived from the air temperature, sea level pressure, and relative humidity (see Bister and Emanuel 2002). Here, the potential intensity is calculated from the surface (1000 hPa) to the tropopause (100 hPa), with 27 levels in ERA-Interim. V_{shear} denotes the magnitude of the VWS between 850 and 200 hPa. Here, the VWS also considers the contribution from meridional winds, defined as the standard deviation of the sum of the zonal and meridional VWS between 850 and 200 hPa. More details can be found in Camargo et al. (2007).

Anomalies in TC further influence TC intensity and track. TCs generating toward the southeast tend to develop into more intense TCs and take early-turning tracks (Camargo and Sobel 2005; Liu and Chan 2008). Hence, we further calculated the ACE and TC occurrence frequency up to the TS intensity. The ACE in a specific grid box with dimensions of $3° \times 3°$ is calculated as the sum of the squares of the maximum sustained surface wind speed of all TCs that emerged within the box, whereas the occurrence frequency indicates the sum of the number of all TCs.

3 Impact of the QBO on Tropical Atmospheric Circulation

We investigated the relationship between U50 and U70 to simply depict the lowest part of the lower stratosphere. As shown in Fig. 1a, the normalized U70 during the TC peak season is highly consistent with the normalized U50 (correlation coefficient: 0.70). Considering that 70 hPa is the nearest level in the lower stratosphere to the tropopause, this level is most suitable to physically explain the stratosphere–troposphere interaction process. Considering that the 70 hPa level is closer to the tropopause than the 50 hPa level, the 70 hPa-defined QBO cases with great amplitudes may exert more significant influence on the troposphere. Wavelet analysis is conducted on the time series of the normalized monthly U70 (shown in Fig. 1b), showing that its dominant period is approximately 26–28 months (the red dashed line denotes 27 months). The global wavelet-test in Fig. 1b shows that U70 can reliably represent the QBO.

To reflect the impact of the QBO on the convection over all of the tropics, the tropical OLR is regressed onto the time series of U70 after removing the ENSO signal, as described in Sect. 2.2 (Fig. 2a). Significant anomalies are observed,

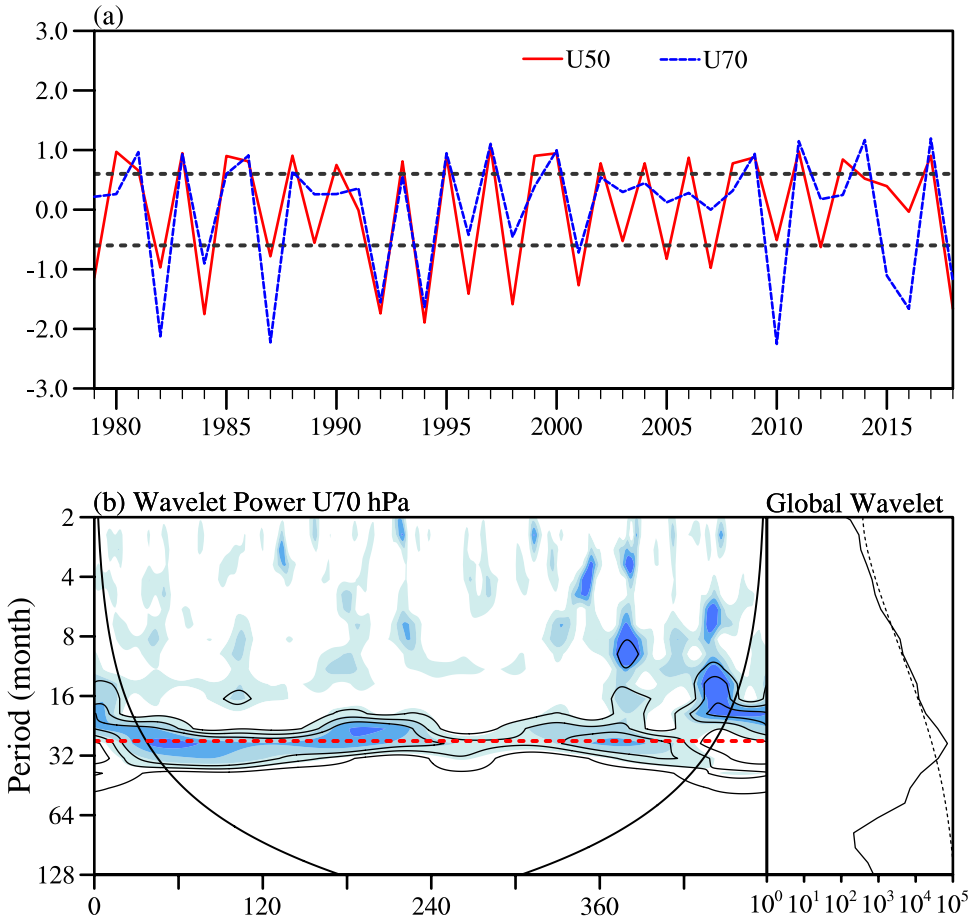

Fig. 1 **a** Time series of the normalized U50 (red solid line) and U70 (blue dashed line) values derived from the FUB-qbo dataset. Horizontal black dashed lines indicate the thresholds of 0.6 and -0.6, which are employed to identify the QBOW and QBOE phases, respectively. **b** Wavelet analysis for U70 during 1979–2018. The thick solid line in the right panel is the global wavelet spectrum for U70, with the dashed line showing the 95% confidence level

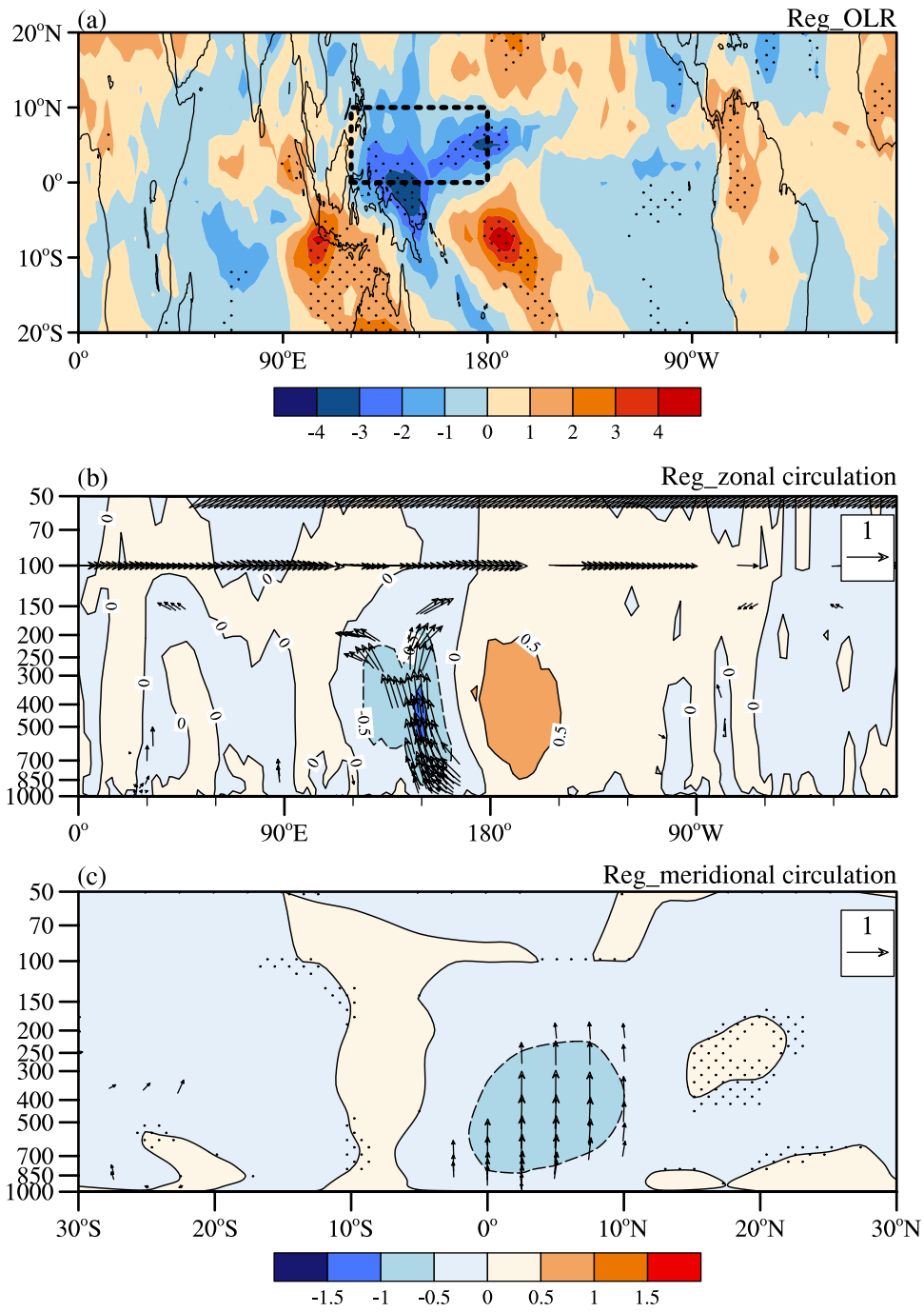

Fig. 2 Anomalies of the **a** OLR (shading; units: W m^{-2}), **b** zonal and vertical velocities averaged between 10° S and 10° N, and **c** meridional and vertical velocities averaged between 120° E and 180° (vectors; units are m s^{-1} for u and 5×10^{-3} Pa s^{-1} for ω; shaded areas indicate the vertical velocity) regressed onto the U70-based QBOres index. The vectors and stippling denote anomalies significant at the 90% confidence level according to Student's t test. The dashed black box in **a** denotes the key region (0°–10° N, 120° E–180°)

with a clear tripole pattern over the tropical Indo-Pacific, and with enhanced convection observed over its central branch (0°–10° N, 120° E–180°) and the inactive convection branches located to both sides (anomalous centers at off-equatorial latitudes in the Southern Hemisphere). Note that the most significant influence from the QBO is concentrated over the WP because deep convection occurs over this region in the boreal TC season. Of greater interest, negative OLR anomalies are observed over the tropical WNP, meaning that convection unimpeded by the cross-tropopause wind shear is expected to occur under the QBOW phase. The negative OLR anomaly center is located on the equator, with wider coverage in the Northern Hemisphere. In contrast, significant positive OLR anomalies are found on both sides of the equator, with greater amplitudes in the Southern Hemisphere. It should be noted that this pattern displays a seasonal dependence with different regression distributions observed in the other seasons.

More details regarding the QBO-tropical convection process can be revealed by analyzing the Walker circulation

response averaged between 10° S and 10° N. As shown in Fig. 2b, a clockwise cell is clearly observed over the CP, with a weaker anticlockwise cell immediately to its left. These three branches are consistent with the tripole pattern exhibited in Fig. 2a. Focusing on the levels above 100 hPa, strong westerlies and westerly shear (westerly winds increase with height) are observed. According to previous studies (e.g., Baldwin et al. 2001; Collimore et al. 2003; Lee et al. 2019), this westerly shear can induce downward motion in the lower-level stratosphere. Generally, the zonal mean vertical velocity is directed downward above 100 hPa (warm colors in Fig. 2b), consistent with previous studies. However, a ventilation opening is observed between 150° E and 180°, where the upward motion in the troposphere can reach up to the lower stratosphere. This ventilation opening might be attributed to the weak VWS between 70 and 200 hPa over the equatorial. These enhanced vertical upward motions are more concentrated in the lower troposphere and split into two parts in the upper troposphere, consistent with the significantly enhanced convection over the tropical WNP under the QBOW phase, as shown in Fig. 2a. The eastern part (150° E–180°) can reach up to the lower stratosphere and the western part (120°–150° E) is mainly observed in the middle troposphere. Affected by the significant upward motion anomalies of the western part, the downward motion anomalies in the upper troposphere (90° E–150° E) are confined between 90° E and 150° E in the lower and middle troposphere.

We further investigate the meridional circulation response averaged between 120° E and 180° (Fig. 2c). In this section, enhanced Hadley circulation is observed under the QBOW phase, with the upward motion branch dominating the equatorial region (between 5° S and 10° N) and a downward motion branch on both sides. Another ventilation opening is detected over 20° N, which should be attributed to lower-level stratospheric pumping induced by the positive vorticity between the equatorial westerly and the off-equatorial prevailing easterly in the lower stratosphere. This process is different from equatorial pumping. In other words, both the narrow pumping along the equator (10° S–10° N, 200–50 hPa) and the wide pumping off the equator (10° N–20° N, 150–50 hPa) contribute to the ventilation between the lower stratosphere and upper troposphere. In addition, downward motion anomalies that suppress off-equatorial convection are observed between 10° N and 25° N in the troposphere. Considering the distribution shown in Fig. 2a, the downward off-equatorial branch is concentrated over the region of 10° N–25° N, 150° E–180°.

The QBO–tropospheric circulation interaction can also be reflected by the regressed conversion rate from the available potential energy (APE) to kinetic energy (KE) in the troposphere considering both the vertical wind and the temperature together. According to Lau and Lau (1992), the conversion of eddy available potential energy (EAPE) into eddy kinetic energy (EKE) indicates the rising motion of warm air parcels and is calculated as $-\frac{R}{P}\,\omega' T'$, where R is the gas constant for dry air, 287 J/(kg K), and P is the pressure at each level (unit: Pascal). The overbar indicates an average over a selected period. Usually, a partial differential is added to ω and T to denote a bandpass filter, thereby extracting some special wave activities from the original data to stress their impacts (e.g., Tsou et al. 2014). In the present study, we retained all the signals caused by the vertical motions of air parcels, calculated the conversion rate from the APE to KE as $-\frac{R}{P}\,\omega T$, and performed vertical integration in the troposphere (between 1000 and 100 hPa; 27 levels in ERA-Interim). As shown in Fig. 3, a similar distribution to that in Fig. 2a is exhibited, with a significant tripole pattern observed over the tropical Indo-Pacific. Positive regressed anomalies over 0°–10° N, 120° E–180° indicate enhanced conversion from the APE into KE; i.e., baroclinic processes provide energy to the deep convection, enabling the convection to rise even higher. In contrast, the off-equatorial region (10°–20° N, 150° E–150° W) shows the opposite

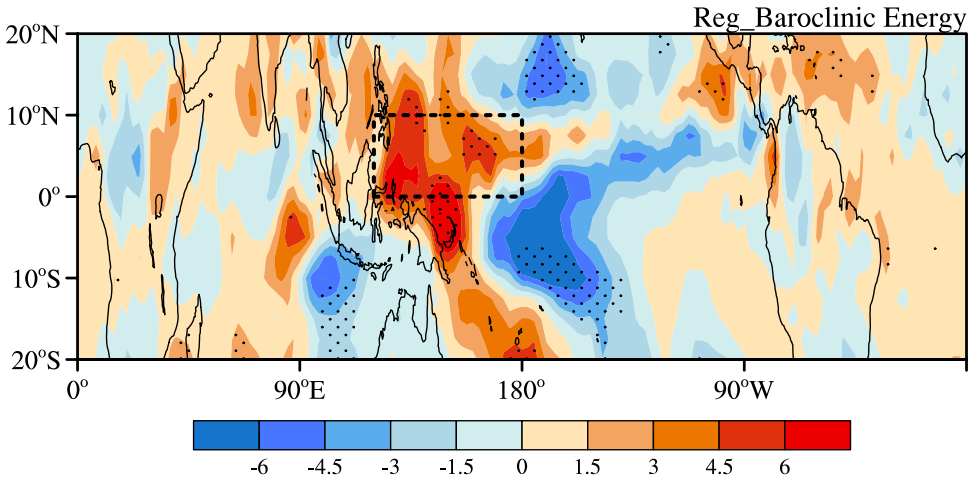

Fig. 3 Anomalies of the vertically integrated conversion rate of APE to KE in the troposphere between 1000 Pa and 100 hPa (shading; units: 10^{-1} W m^{-2}) regressed onto the U70-based QBOres index. The stippling denotes anomalies significant at the 90% confidence level according to Student's t test. The dashed black box denotes the key region (0°–10° N, 120° E–180°)

regressed anomalies, which lead to suppressed impacts on tropospheric processes.

4 Modulation of the QBO on TC Activity

As mentioned above, significant QBO-associated changes in circulations have been observed over the tropical WNP, which is the key region for TC activities. The QBO-associated tropospheric circulation discussed in Sect. 3 may lead to profound changes in both surfaces and surrounding environments, which are influential to TC development. Hence, further investigation focusing on the environmental factors affecting TCs is conducted in Sect. 4. As shown in Fig. 4, the relative vorticity at 850 hPa, divergence at 200 hPa, VWS between 850 and 200 hPa, and mean humidity between 700 and 500 hPa are usually considered to be the most important factors affecting TC genesis (Gray 1968; Feng et al. 2014; Huangfu et al. 2019a). The relative vorticity at 850 hPa regressed onto the U70-based QBOres index (Fig. 4a) is enhanced in the southern part of the MT region in the tropical WNP under the QBOW phase. However, negative relative vorticity anomalies are observed in the northern part, leading to the opposite influence on TC genesis. This distribution may be reinforced by the upper-level divergence, as shown in Fig. 4b. The divergence anomalies at 200 hPa cover a large extent of the southern WNP; the most significant region is that within 0°–10° N, 120° E–150° E. This distribution is consistent with the regressed wind field shown in Fig. 2b. Moreover, the VWS is calculated and regressed onto the QBOres index (Fig. 4c). The VWS distribution resembles that of the relative vorticity shown in Fig. 4a, with the most significant weak VWS anomalies concentrated over the southeast quadrant of the tropical WNP. In

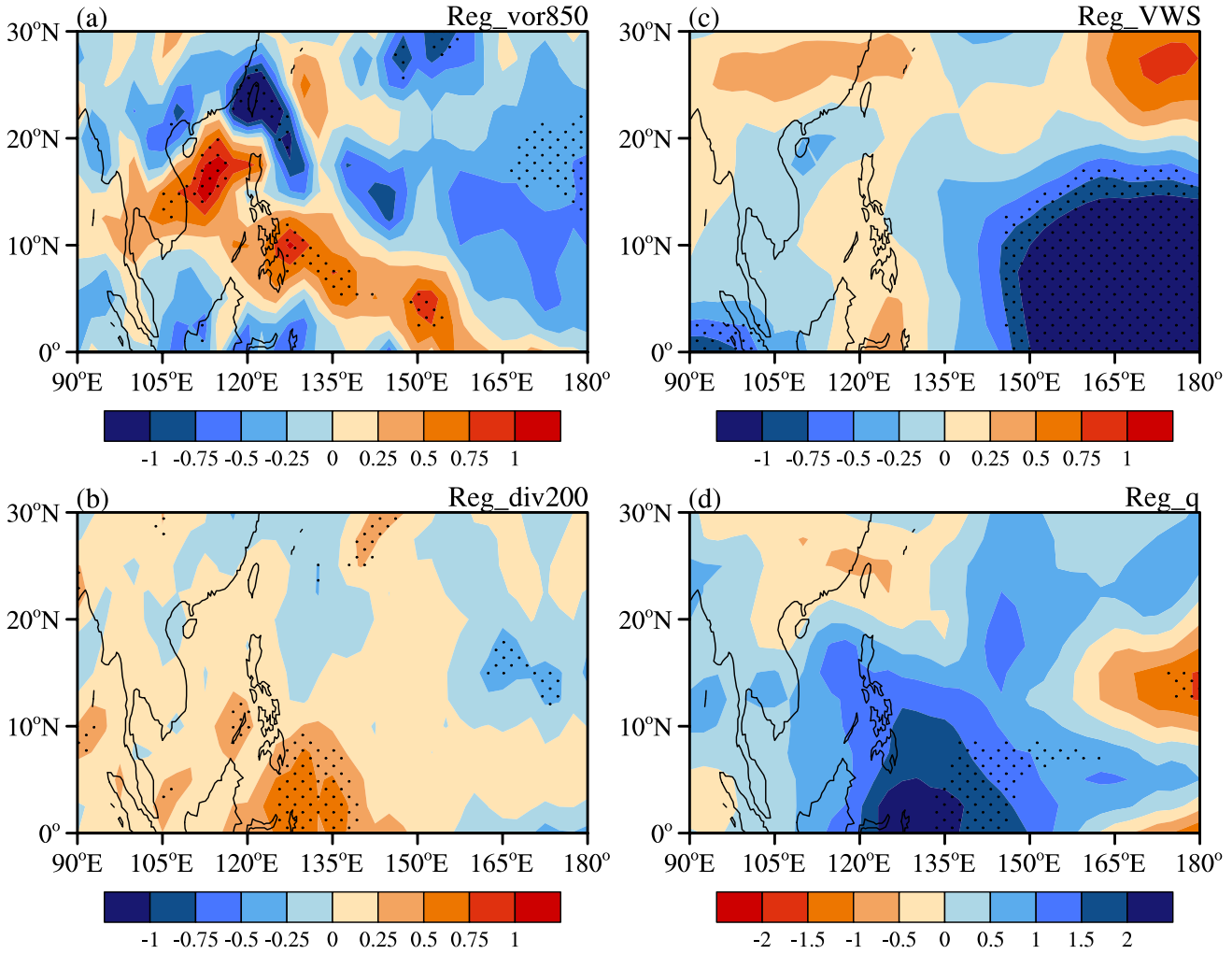

Fig. 4 Anomalies of the **a** 850 hPa relative vorticity (units: 10^{-6} s^{-1}), **b** 200 hPa divergence (units: 10^{-6} s^{-1}), **c** 200–850 hPa VWS (units: m s^{-1}) and **d** mean relative humidity between 700 and 500 hPa (units: %) regressed onto the U70-based QBOres index. The stippling denotes anomalies significant at the 90% confidence level according to Student's t test

addition, mid-level moisture provides important support to TC genesis. As shown in Fig. 4d, enhanced relative humidity anomalies are observed in the southern WNP, favoring TC genesis in this region. Similar to the dynamic factors, the region from 10° N to 25° N, 150° E to 180° bears the opposite anomalies.

We further calculate the thermodynamic GPI considering all of the above four factors together (Camargo et al. 2007). However, the humidity (*H*) term in the GPI equation employs the relative humidity at 600 hPa (500–700 hPa mean in Fig. 4d). As shown in Fig. 5, positive GPI anomalies are observed along the MT region, especially over its southern part (0°–10° N, 120° E–180°; solid box in Fig. 5), meaning that more TCs are probably generated here under the QBOW phase. Note that GPI used here is also preprocessed, with the ENSO signals have been removed. In contrast, significant negative GPI anomalies are observed in the northern tropical WNP (10°–25° N, 150° E–180°; dashed box in Fig. 5), presenting suppressed TC genesis trends. The regions within these two boxes are the most important regions of TC genesis, and the areas of the boxes are selected based on both the significance shown in Fig. 5 and the QBO-induced circulation anomalies depicted in Fig. 2.

Gray (1984) suggested that the TCs over the Atlantic are associated with trade easterlies, whereas the TCs generated over the WNP are related to the MT. Hence, we composited the MT anomalies in both the QBOW and the QBOE phases (represented by the relative vorticity at 850 hPa; shaded in Fig. 6). The composite years are selected based on the time series of the normalized U70res, as illustrated in Sect. 2. Eleven QBOW cases are identified, namely, 1981, 1983, 1986, 1995, 1997, 2000, 2002, 2009, 2011, 2014 and 2017; ten QBOE cases are identified, namely, 1982, 1984, 1987, 1992, 1994, 2001, 2010, 2015, 2016, and 2018. Based on the JASO mean Niño 3.4 index, we removed strong El Niño and La Niña cases from the QBOW and QBOE groups. Nine QBOW cases (1981, 1983, 1986, 1995, 2000, 2009, 2011, 2014, and 2017) and six QBOE cases (1984, 1992, 1994, 2001, 2016, and 2018) are employed to conduct the composite analysis in this study. As shown in Fig. 6a, a meridional contrast is observed, with the southern (northern) part of the MT enhanced (weakened) under the QBOW phase. The positive anomalies of the relative vorticity show an eastward extension of the MT, while the off-equatorial region exhibits a negative response to the QBO modulation. In contrast, the MT generally shows opposite anomalies in the QBOE phase, consistent with the analysis in Fig. 4a. Further, the TCs within the boxes shown in Fig. 5 (above

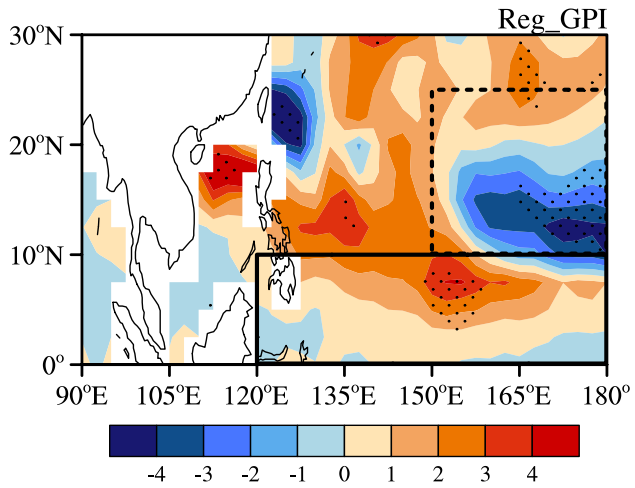

Fig. 5 Anomalies of the GPI (units: %) regressed onto the U70-based QBOres index. The stippling denotes anomalies significant at the 90% confidence level according to Student's t test. The solid black box denotes the key region (0°–10° N, 120° E–180°), and the dashed black box denotes the adjacent northern region (10° N–25° N, 150° E–180°)

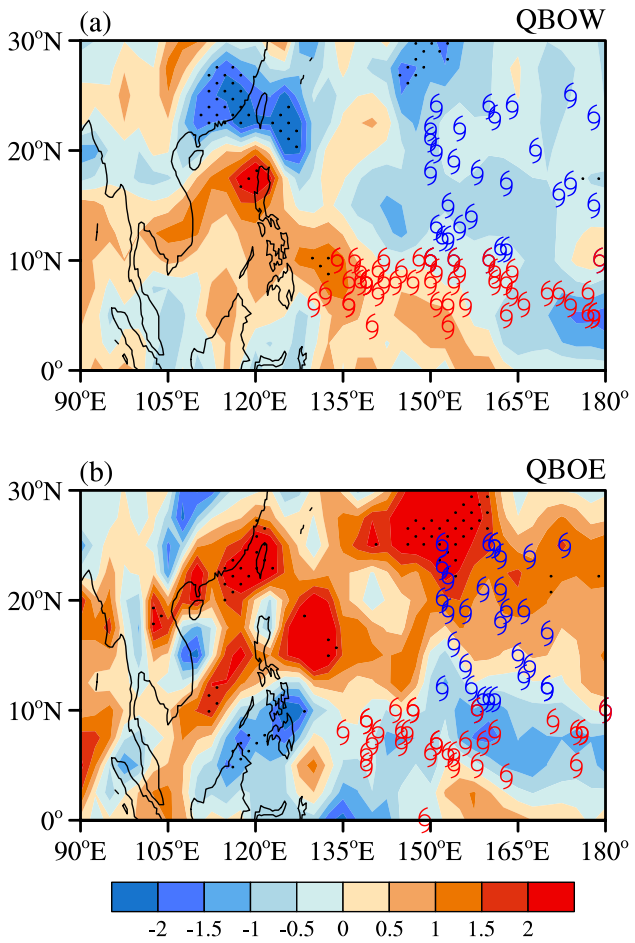

Fig. 6 Composited 850 hPa vorticity anomalies (units: 10^{-6} s^{-1}) for the **a** QBOW and **b** QBOE phases. Stippling denotes anomalies significant at the 90% confidence level according to Student's t test. The typhoon symbols indicate the locations of TCs generated in the southern key region (red symbols) and the northern region (blue symbols), as shown in Fig. 5

the TS level) are superimposed in Fig. 6. The TCs generated in the southern box (red TC symbols) in the QBOW phase occur more frequently in the eastern part than the TC in the QBOE phase, especially east of 160° E. Additionally, the annual number of TCs generated in the QBOW phase is 5.4 (49 TCs generated in 9 cases), slightly more than that in the QBOE phase (5.3; 32 TCs generated in 6 cases). However, due to the diverse anomalies in the northern part of the MT region, the annual number of TCs generated in the QBOW phase (3.4; 31 TCs in 9 cases) is less than that in the QBOE phase (5.3; 32 TCs in 6 cases). This tendency corroborates previous studies (e.g., Wu et al. 2012) in which more TCs tend to be generated over the eastern tropical WNP when the MT extends eastward. As shown in Table 1, we have calculated the correlation coefficients between the QBOres index (including different levels: 70, 50, 40, 30, 20, and 10 hPa) and TC numbers (including three different levels: tropical depression, tropical storm, and typhoon) based on the datasets during the period from 1979 to 2018, with updated 10-year data. The correlation between the QBO and TC numbers over the WNP is still not statistically significant at the 90% confidence level, which is consistent with the result based on the period from 1983 to 2008, with no more decadal changes observed. However, the correlation analysis may not be appropriate enough to examine the QBO–TC relationship. Future studies focusing on specific regions with updated data may still conclude meaningful results. In addition, the modulation effect of QBO might be different when coupled with different tropospheric events.

In the TC peak season, the MT dominates the tropical region over the WNP. The northeast side of the MT (southeasterlies) is adjacent to the southwest rim of the western Pacific subtropical high (WPSH). In other words, the relative vorticity anomalies in Fig. 6a also show the retreat of the WPSH, concurrent with the eastward extension of the MT, which is influential to the tracks of TCs (Ho et al. 2009). Ho et al. (2009) revealed significant changes in the TC tracks outside the tropics under different QBO phases with a zonal dipole pattern observed in the band between 25° N and 35° N. With updated data, we analyzed the corresponding changes in the TC tracks based on the regression on the U70-defined QBOres index (c.f., Ho et al. 2009 employed the VWS between 50 and 70 hPa as the QBO index). As shown in Fig. 7a, the ACE of TCs is calculated in each 3° × 3° box over the WNP and regressed onto the QBOres index. Considering that weak ACE accumulates in the southern part of the tropical WNP, most regressed signals are observed off 10° N. Significant negative ACE anomalies are observed along the northern part of the MT, showing a significant influence on TC tracks toward Taiwan. In contrast, the positive ACE anomalies in the South China Sea and East China Sea show an opposite response to the QBOW phase. The ACE anomalies to the north of 25° N are consistent with the study of Ho et al. (2009). Further, we calculated the TC occurrence frequency and obtained a similar distribution. The results shown in Fig. 7b indicate that the ACE anomalies can mostly be explained by changing TC tracks. As reported by Gray et al. (2018), the intertropical convergence zone (ITCZ) shifts southward under the QBOW phase, as does the MT. Therefore, the TC tracks shift southward accordingly, and more TC tracks would move toward Taiwan under the QBOE phase. The distributions in Fig. 7a,b are consistent with the results in Fig. 6. The positive ACE anomalies and more frequent TC in the QBOE phase are significant in the northern part of the MT region, which can be explained predominantly by the enhanced TC genesis in the off-equatorial eastern WNP (Fig. 6b). The shift of TC tracks toward Taiwan under the QBOE phase can improve the seasonal forecasts of TC activity over the surrounding regions.

Table 1 Correlation coefficients between the QBO index (U70, U50, U40, U30, U20, and U10 hPa) and TC numbers (including three different levels: tropical depression, NTC; tropical storm, NTS; typhoon, NTY)

Indices	U70	U50	U40	U30	U20	U10
WNP_NTC	− 0.15	− 0.25	− 0.14	− 0.02	0.02	0.03
SWNP_NTC	0.07	0.00	0.05	0.04	− 0.03	− 0.19
NWNP_NTC	− 0.08	− 0.14	− 0.05	0.04	0.03	− 0.05
WNP_NTS	− 0.07	− 0.13	− 0.07	− 0.03	− 0.07	− 0.07
SWNP_NTS	0.09	0.05	0.07	0.04	− 0.06	− 0.24
NWNP_NTS	− 0.03	− 0.07	− 0.01	0.02	− 0.04	− 0.13
WNP_NTY	− 0.23	− 0.25	− 0.21	− 0.08	0.10	0.22
SWNP_NTY	0.05	0.02	0.02	0.02	0.01	− 0.12
NWNP_NTY	− 0.11	− 0.12	− 0.09	− 0.02	0.04	0.04

WNP denotes the region within 0°–30°N, 120°E–180°, SWNP denotes the region within 0°–10°N, 120°E–180°, and NWNP denotes the region within 10°–25°N, 150°E–180°, respectively

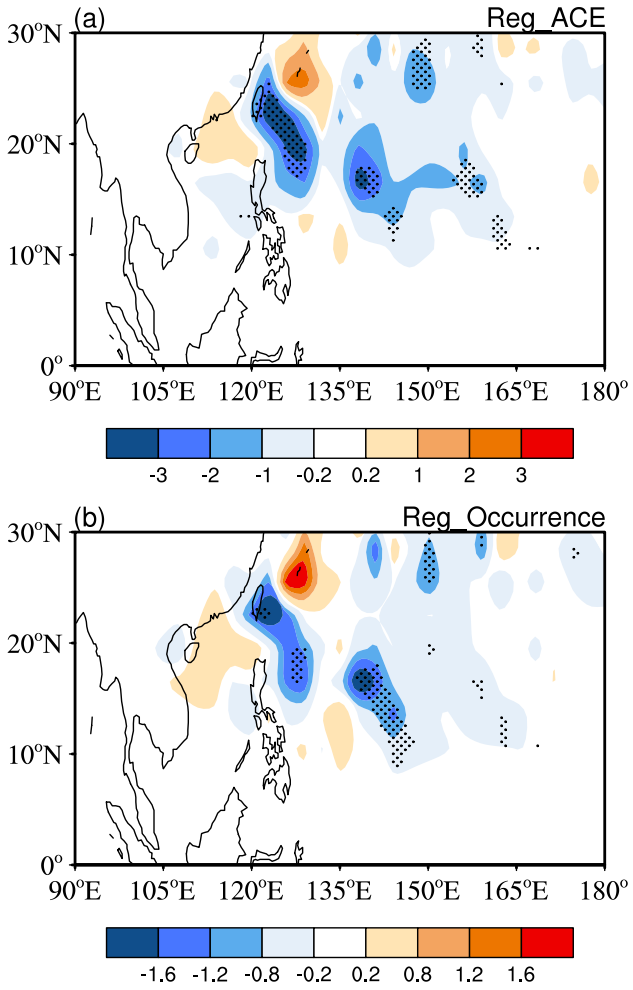

Fig. 7 Anomalies of the **a** ACE (in a 3°×3° box; unit: 10^3 m^2 s^{-2}) and **b** frequency of TC occurrence (in a 3°×3° box) regressed onto the U70-based QBOres index. The stippling denotes anomalies significant at the 90% confidence level according to Student's t test

5 Summary and Discussion

Based on the findings in the present study, a schematic is summarized in Fig. 8 to provide a clearer and updated overview of the QBO–troposphere interaction process over the Pacific. The climatological mean fields are shown in gray, and the colored shapes are associated with the QBO phases. Following Gray et al. (2018), we employed 70 hPa as the critical level of the QBO, with Fig. 8a (8b) showing the state in the QBOW (QBOE) phase. At this level, the QBO is zonally homogeneous and centered on the equator (westerlies, red vectors; Belmont and Dartt 1968; Wallace 1973). Within the tropical region in the Northern Hemisphere, the westerlies over the equator and the easterlies over the off-equatorial region can form a cyclonic band, providing an upwelling force to the tropopause (c.f., Fig. 2c). Although this force is treated as zonally homogeneous, the effect of this force is quite different when considering the underlying upper-tropospheric winds. According to the climatological mean state of the zonal wind in the upper-troposphere along the equator, which is the upper-level region of the Pacific Walker circulation, as shown at 200 hPa, notable westerlies (or weak easterlies in some years) can be observed over the CP, with the WP and eastern Pacific (EP) both controlled by easterlies (Ma and Zhou 2016). Hence, the weak VWS between 70 and 200 hPa over the equatorial CP reinforces the upward motion anomalies (blue vector; c.f., Fig. 2b). Therefore, with both the stratospheric pumping and the force from the equatorial VWS, the convection over the eastern WNP within the off-equatorial region is enhanced due to the influence of the QBO, leading to a higher tropopause (thick blue curve). In contrast, the stronger VWS on both sides of the upward branch leads to suppressed vertical motions over the equator (red vectors). Based on the results in the present study, we found approximately opposite anomalies during the QBOE phase (Fig. 8b).

After revisiting the anomalies in the QBO-associated circulations, we examined the corresponding changes in TC activities over the WNP. Although significant circulation anomalies are also observed on both sides of the WNP, TC activities are not active in these regions, especially in the Southern Hemisphere. Hence, we focus mainly on the TC activities in the WNP. Concurrent with the QBOW phase, a favorable environment for TC genesis is observed along the southern MT, yet the northern MT is unfavorable for TC genesis. Considering the QBO-associated circulation anomalies, we conducted statistical analysis, the results of which reveal that under the QBOW phase, more TCs tend to generate in the equatorial region of the WNP, whereas fewer TCs are generated in the off-equatorial region over the WNP. All levels of TCs (TD, TS, and typhoon) show consistent trends. Moreover, the TC tracks show significant changes under different QBO phases. Concomitant with the QBOE phase, the MT shifts northward, and more TCs occur closer to Taiwan. These results may add more tropical signals to the study of Ho et al. (2009).

The main purpose of the present study is to reveal the different modulation effects of the QBO on the troposphere in the zonal direction. With greater convective activities over the WP, a significant response to stratospheric ventilation is observed. With the ventilation opening located over the western CP, the QBOW phase shows a westward-tilted pumping effect on convections due to the prevailing easterlies in the upper troposphere. In addition to the focus on TC activities in the present study, additional tropical events should be reexamined to discern their relationship with QBO events, especially over the WNP. Moreover, the present study focuses mainly on the central branch of the tripole pattern mentioned in the regressed convection anomalies. The impacts exerted by both sides have still not been

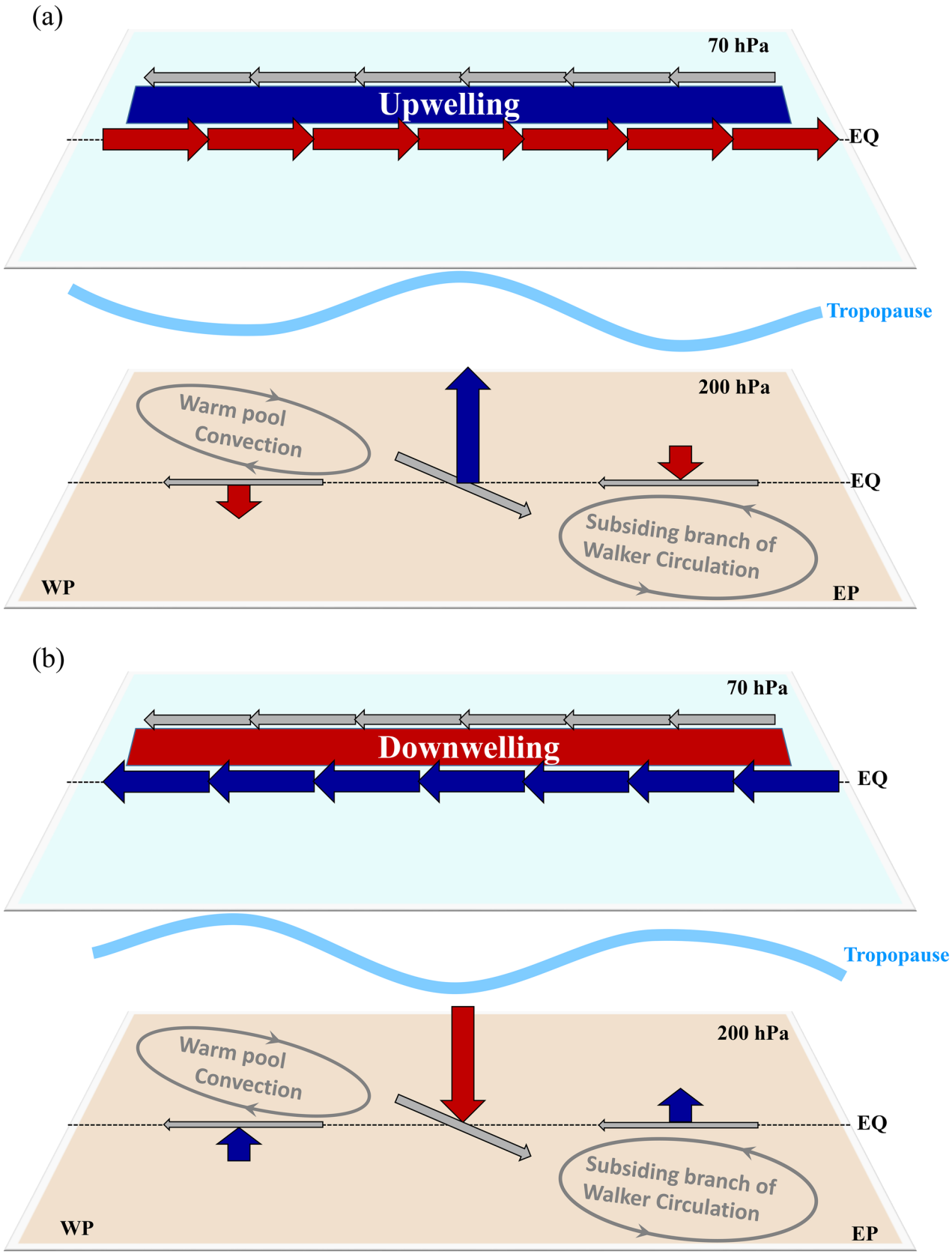

Fig. 8 Schematic diagram of the impacts of the **a** QBOW and **b** QBOE phases on tropical convection over the Pacific

Table 2 Correlation coefficients between the QBO index (U70, U50, U40, U30, U20, and U10 hPa) and ENSO indices (Niño 3 index, Niño3.4 index, Niño 4 index and EMI) based on monthly data in JASO during the period 1979–2018

Indices	Niño 3	Niño 34	Niño 4	EMI
U70	− 0.05	− 0.09	− 0.09	− 0.11
U50	0.07	0.03	− 0.02	− 0.09
U40	0.13	0.09	0.03	− 0.05
U30	0.20	0.19	0.14	0.07
U20	0.24	0.26	0.24	0.18
U15	0.19	0.22	0.20	0.16
U10	0.10	0.13	0.11	0.08

thoroughly discussed under different QBO phases. Additionally, the influence of the QBO on TC activity is limited. Further studies should be carried out to study the combined impacts of the QBO and the tropical Indian Ocean, which is considered to be the dominant factor influencing boreal summertime TCs (Zhan et al. 2011, 2014; Ha et al. 2015; Huangfu et al. 2019a).

In addition, we calculated the correlation coefficients between the QBO index (seven levels in FUB-qbo: 70 hPa, 50 hPa, 40 hPa, 30 hPa, 20 hPa, 15 hPa and 10 hPa zonal winds) and ENSO indices [Niño 3 index, Niño 3.4 index, Niño 4 index and El Niño Modoki Index (EMI)] based on monthly data in JASO during the period 1979–2018. The correlation coefficients are not statistically significant in this period (Table 2), indicating that the regression results based on the residual data bear great resemblance to those based on the original data. As has been discussed in previous studies (c.f., page L06702 in Ho et al. 2009 or page 5816 in Camargo and Sobel 2010), the QBO–TC activity relationship is essentially unchanged after removing the ENSO signal. Additionally, previous studies always treated the QBO effects as symmetric along the equator, although some reanalysis data oppose this notion. Perhaps future research can provide systematic and convincing observational data above the tropopause, with which we can conduct meaningful studies on the asymmetric impacts of the QBO.

Acknowledgements This work was supported by the National Key Research and Development Program of China (2018YFC1506003), the Key Program of the Chinese Academy of Sciences (Grant QYZDY-SSW-DQC024) and the National Natural Science Foundation of China (Grant no. 41705071). The authors are grateful for the comments and suggestions provided by the editor and anonymous reviewers.

References

Angell JK, Korshover J (1964) Quasi-biennial variations in temperature, total ozone, and tropopause height. J Atmos Sci 21:479–492

Baldwin MP et al (2001) The quasi-biennial oscillation. Rev Geophys 39:179–229

Bell GD et al (2000) Climate Assessment for 1999. Bull Am Meteorol Soc 81:S1–S50

Belmont AD, Dartt DG (1968) Variation with longitude of the quasi-biennial oscillation. Mon Weather Rev 96:767–777

Bister M, Emanuel KA (2002) Low frequency variability of tropical cyclone potential intensity 1. Interannual to interdecadal variability. J Geophys Res Atmos 107:2621–2615

Camargo SJ, Sobel AH (2005) Western North Pacific tropical cyclone intensity and ENSO. J Clim 18:2996–3006

Camargo SJ, Sobel AH (2010) Revisiting the influence of the quasi-biennial oscillation on tropical cyclone activity. J Clim 23:5810–5825

Camargo SJ, Emanuel KA, Sobel AH (2007) Use of a genesis potential index to diagnose ENSO effects on tropical cyclone genesis. J Clim 20:4819–4834

Chan JCL (1995) Tropical Cyclone activity in the Western North Pacific in relation to the stratospheric quasi-biennial oscillation. Mon Weather Rev 123:2567–2571

Chen W, Feng J, Wu R (2013) Roles of ENSO and PDO in the link of the East Asian Winter Monsoon to the following summer monsoon. J Clim 26:622–635

Collimore CC et al (2003) On the relationship between the QBO and tropical deep convection. J Clim 16:2552–2568

Emanuel KA, Nolan DS (2004) Tropical cyclone activity and the global climate system. Proc. 26th Conf. on Hurricanes and Tropical Meteorology, Miami, FL, Amer. Meteor. Soc., 10A.2. https://ams.confex.com/ams/26HURR/techprogram/paper_75463.htm

Fadnavis S, Chakraborty T, Ghude SD, Beig G, Ernest Raj P (2011) Modulation of Cyclone tracks in the Bay of Bengal by QBO. J Atmos Solar Terr Phys 73:1868–1875

Fadnavis S, Ernest Raj P, Buchunde P, Goswami BN (2014) In search of influence of stratospheric quasi-biennial oscillation on tropical cyclones tracks over the Bay of Bengal region. Int J Climatol 34:567–580

Feng T, Chen G-H, Huang R-H, Shen X-Y (2014) Large-scale circulation patterns favourable to tropical cyclogenesis over the western North Pacific and associated barotropic energy conversions. Int J Climatol 34:216–227

Giorgetta MA, Bengtsson L, Arpe K (1999) An investigation of QBO signals in the east Asian and Indian monsoon in GCM experiments. Clim Dyn 15:435–450

Gray WM (1968) Global view of the origin of tropical disturbances and storms. Mon Weather Rev 96:669–700

Gray WM (1984) Atlantic seasonal hurricane frequency. Part I: El Niño and 30 mb quasi-biennial oscillation influences. Mon Weather Rev 112:1649–1668

Gray WM (1988) Environmental influences on the tropical cyclones. Aust Meteorol Mag 36:127–139

Gray WM, Sheaffer JD, Knaff JA (1992) Influence of the stratospheric QBO on ENSO variability. J Meteorol Soc Jpn 70:975–995

Gray LJ, Anstey JA, Kawatani Y, Lu H, Osprey S, Schenzinger V (2018) Surface impacts of the quasi biennial oscillation. Atmos Chem Phys 18:8227–8247

Ha Y, Zhong Z, Yang X, Sun Y (2015) Contribution of East Indian Ocean SSTA to Western North Pacific tropical cyclone activity under El Niño/La Niña conditions. Int J Climatol 35:506–519

Ho C-H, Kim H-S, Jeong J-H, Son S-W (2009) Influence of stratospheric quasi-biennial oscillation on tropical cyclone tracks in the western North Pacific. Geophys Res Lett. https://doi.org/10.1029/2009gl037163

Huang B, Hu Z-Z, Kinter JL, Wu Z, Kumar A (2012) Connection of stratospheric QBO with global atmospheric general circulation and tropical SST. Part I: methodology and composite life cycle. Clim Dyn 38:1–23

Huangfu J, Chen W, Huang R, Feng J (2019a) Modulation of the impacts of the Indian Ocean Basin mode on tropical cyclones

over the Northwest Pacific during the boreal summer by La Niña Modoki. J Clim 32:3313–3326
Huangfu J, Chen W, Jian M, Huang R (2019b) Impact of the cross-tropopause wind shear on tropical cyclone genesis over the Western North Pacific in May. Clim Dyn 52:3845–3855
Huesmann AS, Hitchman MH (2001) The stratospheric quasi-biennial oscillation in the NCEP reanalyses: climatological structures. J Geophys Res Atmos 106:11859–11874
Knapp KR, Kruk MC, Levinson DH, Diamond HJ, Neumann CJ (2010) The international best track archive for climate stewardship (IBTrACS) unifying tropical cyclone data. Bull Am Meteorol Society 91:363–376
Knapp KR, Diamond HJ, Kossin JP, Kruk MC, Schreck CJ III (2018). International best track archive for climate stewardship (IBTrACS) Project, Version 4.v04r00. NOAA National Centers for Environmental Information. https://doi.org/10.25921/82ty-9e16
Lau K-H, Lau N-C (1992) The energetics and propagation dynamics of tropical summertime synoptic-scale disturbances. Mon Weather Rev 120:2523–2539
Lee J-H, Kang M-J, Chun H-Y (2019) Differences in the tropical convective activities at the opposite phases of the quasi-biennial oscillation. Asia Pac J Atmos Sci 55:317–336
Liang W, Jian M, Qiao Y (2012) Relationship between QBO and the onset of south China sea summer monsoon. J Trop Meteorol 28:237–242
Liebmann BCAS (1996) Description of a complete (interpolated) outgoing longwave radiation dataset. Bull Am Meteorol Soc 77:1275–1277
Liu KS, Chan JC (2008) Interdecadal variability of western North Pacific tropical cyclone tracks. J Clim 21:4464–4476
Ma S, Zhou T (2016) Robust strengthening and westward shift of the tropical Pacific Walker circulation during 1979–2012: a comparison of 7 sets of reanalysis data and 26 CMIP5 models. J Clim 29:3097–3118
Rayner N et al (2003) Global analyses of sea surface temperature, sea ice, and night marine air temperature since the late nineteenth century. J Geophys Res Atmos 108(D14):4407. https://doi.org/10.1029/2002JD00267
Reed R et al (1961) Evidence of a downward propagating annual wind reversal in the equatorial stratosphere. J Geophys Res 66:813–818
Shapiro LJ (1989) The relationship of the quasi-biennial oscillation to Atlantic tropical storm activity. Mon Weather Rev 117:1545–1552
Simmons A, Uppala S, Dee D, Kobayashi S (2007) ERA-interim: new ECMWF reanalysis products from 1989 onwards. ECMWF Newsl 110:25–35
Tsou C-H, Hsu H-H, Hsu P-C (2014) The role of multiscale interaction in synoptic-scale Eddy kinetic energy over the western North Pacific in Autumn. J Clim 27:3750–3766
Wallace JM (1973) General circulation of the tropical lower stratosphere. Rev Geophys 11:191–222
Wang L, Chen W, Huang R (2007) Changes in the variability of North Pacific Oscillation around 1975/1976 and its relationship with East Asian winter climate. J Geophys Res Atmos. https://doi.org/10.1029/2006jd008054
Wu L, Wen Z, Huang R, Wu R (2012) Possible linkage between the monsoon trough variability and the tropical cyclone activity over the Western North Pacific. Mon Weather Rev 140:140–150
Xue X, Chen W, Chen S, Zhou D (2015) Modulation of the connection between boreal winter ENSO and the South Asian high in the following summer by the stratospheric quasi-biennial oscillation. J Geophys Res Atmos 120:7393–7411
Zhan R, Wang Y, Wu C-C (2011) Impact of SSTA in the East Indian Ocean on the frequency of northwest Pacific Tropical cyclones: a regional atmospheric model study. J Clim 24:6227–6242
Zhan R, Wang Y, Tao L (2014) Intensified impact of East Indian Ocean SST anomaly on tropical cyclone genesis frequency over the western North Pacific. J Clim 27:8724–8739
Zhang J et al (2019) Seasonal evolution of the quasi-biennial oscillation impact on the Northern Hemisphere Polar Vortex in Winter. J Geophys Res Atmosp 124:12568–12586